Isotactic Polypropylene Hollow Microfibers Prepared by CO_2 Laser-Thinning

Akihiro Suzuki, Hiroshi Ohnishi

Interdisciplinary Graduate of School of Medicine and Engineering, University of Yamanashi, Kofu 400-8511, Japan

Received 31 January 2005; accepted 6 May 2006
DOI 10.1002/app.24699
Published online in Wiley InterScience (www.interscience.wiley.com).

ABSTRACT: An isotactic polypropylene hollow microfiber was continuously produced by using a carbon dioxide (CO_2) laser-thinning method. To prepare the hollow microfiber continuously, the apparatus used for the thinning of the solid fiber was improved so that the laser can circularly irradiate to the hollow fiber. Original hollow fiber with an outside diameter (OD) of 450 μm and an internal diameter (ID) of 250 μm was spun by using a melt spinning machine with a specially designed spinneret to produce the hollow fiber. An as-spun hollow fiber was laser-heated under various conditions, and the OD and the ID decreased with increasing the winding speed. For example, when the hollow microfiber obtained by irradiating the CO_2 laser to the original hollow fiber supplied at 0.30 m min^{-1} was wound up at 800 m min^{-1}, the obtained hollow microfiber had an OD of 6.3 μm and an ID of 2.2 μm. The draw ratio calculated from the supplying and the winding speeds was 2667-fold. The hollow microfibers obtained under various conditions had the hollowness in the range of 20–30%. The wide-angle X-ray diffraction patterns of the hollow microfibers showed the existence of the highly oriented crystallites. Further, the OD and ID decreased, and the hollowness increased by drawing hollow microfiber obtained with the laser-thinning. © 2006 Wiley Periodicals, Inc. J Appl Polym Sci 102: 2600–2607, 2006

Key words: poly(propylene); hollow microfibers; laser-thinning

INTRODUCTION

Hollow fibers have been produced by various polymers, such as an isotactic polypropylene (i-PP),[1] poly (ethylene terephthalate) (PET),[2] poly(ether ether ketone),[3] and polysulfone,[4] and their properties have been studied by a large number of researchers. The i-PP hollow fiber is particularly studied from various viewpoints such as melt spinning, drawing, filtration properties, etc.[5,6] The i-PP hollow fiber can be used for special end uses such as membranes and artificial kidneys because a microporous structure is induced by annealing and drawing the i-PP hollow fiber.[7]

The hollow fibers, usually used, have their diameters ranging from 200 to 300 μm, and its diameter is ten times larger than that of solid fibers. It is difficult to make the hollow microfiber from technical point of view because the spinning techniques,[8–11] such as a conjugate spinning and an islands-in-a-sea type fiber spinning, to produce the solid microfibers cannot make the microfiber with hollow structure.

It was found that microfibers were prepared by irradiating a carbon dioxide (CO_2) laser to solid fibers. The apparatus developed in our laboratory to continuously prepare the microfibers can wind up the microfiber as a monofilament in the winding speed range of 100–2500 m min^{-1}. The laser-thinning method was already applied to the PET,[12] nylon 6[13] and the i-PP fibers,[14] poly(L-lactic acid),[15] and poly(glycolic acid) fibers to make their microfibers. The obtained microfiber had a diameter of 1–5 μm.

The CO_2 laser-thinning method gives easily the microfibers of various polymers without especially highly skilled techniques when compared with the especially highly skilled techniques such as a conjugate spinning, an islands-in-a-sea type fiber spinning, a melt blowing, and a flash spinning. In the laser thinning, the temperature of the fiber irradiating the CO_2 laser beam instantly reaches near its melting temperature (T_m), and the melt viscosity in the part of the fiber heated becomes sufficiently low without elongation or cutting, and the heated part enters nearly a molten state. The fiber is continuously thinned by the plastic flow occurring from the nearly molten state, and then the microfiber, having fallen down because of its own weight, is wound on the winding spool. The instantaneous plastic flow at a high strain rate induces the molecular orientation and crystallization despite a large deformation, just like in flow drawing, and gives an oriented microfiber. The laser-thinning occurred an instantaneous large deformation differs largely from conventional drawings and melt spinnings in deformation process.

Correspondence to: A. Suzuki (a-suzuki@yamanashi.ac.jp).

Journal of Applied Polymer Science, Vol. 102, 2600–2607 (2006)

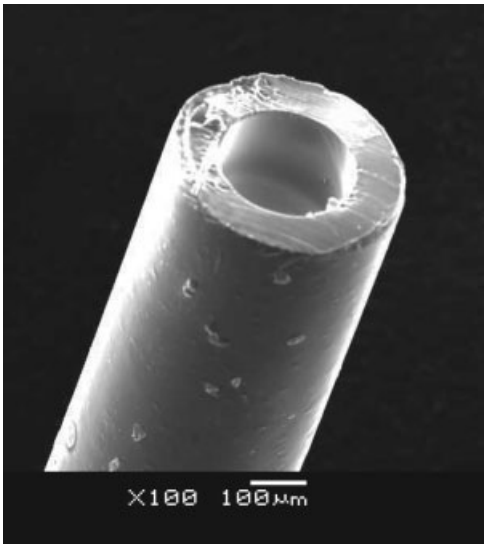

Figure 1 SEM photograph of original i-PP hollow fiber.

In this study, the i-PP hollow microfibers were produced by laser-thinning carried out under various conditions. We present here the results pertaining to the properties of the i-PP hollow microfiber obtained by using the improved apparatus.

EXPERIMENTAL

Material

The hollow fibers were produced from commercial grade i-PP pellets by using a laboratory-scale melt extruder with a tube-in-orifice spinneret. Nitrogen gas was injected in the center of the molten filament to produce the hollow structure. Its tacticity was highly isotactic, $\sim$ 96%, which was determined by using nuclear magnetic resonance techniques. The original hollow fiber having an outside diameter (OD) of 450 μm and an internal diameter (ID) of 250 μm was spun at a spinning temperature of 230°C, and had a degree of crystallinity of 45.9% estimated from heat of fusion. The original hollow fiber had a hollowness (h) of 32% and a tube wall with a uniform thickness as shown in Figure 1. The h value is the percentage void in the cross section and is defined as $h\,(\%) = (\mathrm{ID}/\mathrm{OD})^2 \times 100$.

As-spun hollow fibers were found to be slightly oriented from wide-angle X-ray diffraction images as shown in Figure 2.

Measurements

The OD and ID of hollow microfiber were measured by a scanning electron micrograph (SEM). SEM was observed on a JSM6060LV (JEOL, Japan) with an acceleration voltage of 19 kV.

Wide-angle X-ray diffraction (WAXD) images were taken using an imaging-plat reader (Rigaku, Japan). The imaging-plate was attached to a Rigaku X-ray generator (Rigaku, Japan) that was operated at 36 kV and 18 mA. The radiation used was Ni-filtered Cu Kα. The sample to imaging-plat distance was 40 mm. The hollow microfiber was exposed for 20 min to the X-ray beam from a pinhole collimator with a diameter of 0.4 mm.

The degree of crystal orientation (π) was estimated from the half-width (H) of the meridian reflection peak. The H value was estimated from WAXD pattern measured by the imaging-plate through the software for analyzing data.

The π value is given by the equation:

$$\pi(\%) = [(180 - H)/180] \times 100$$

Differential scanning calorimetry (DSC) measurements were carried out using a Rigaku THERM PLUS 2 DSC 8230C calorimeter. The DSC scans were performed within the temperature range of 25–180°C, using a heating rate of 10°C min^{-1}. All DSC experiments were carried out under a nitrogen purge. The DSC instrument was calibrated with indium.

The degree of crystallinity (X_c) was determined from heat of fusion (ΔH_m) as follows:

$$X_c(\%) = [\Delta H_m/\Delta H_m^0] \times 100$$

where the heat of fusion of the crystalline phase (ΔH_m^0) is 146.5 J g^{-1}.[16]

A thermal mechanical analysis (TMA) was carried out with a THERM PLUS TMA8310 (Rigaku, Akishima, Japan) at a heating rate of 5°C min^{-1}. The measurements were performed over the temperature range from 25 to 175°C. The specimens (15 mm long) were given a very small tension (5 mN) to stretch the specimen tightly.

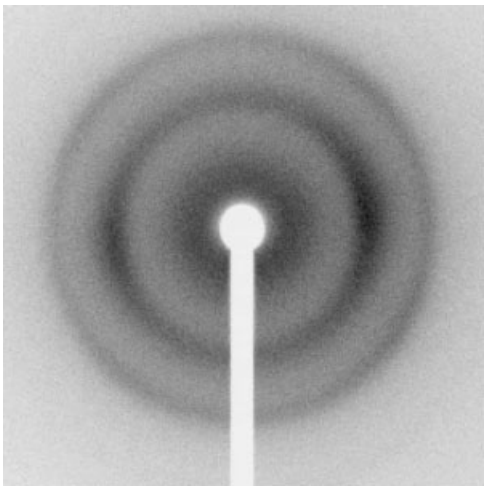

Figure 2 Wide-angle X-ray diffraction pattern of original i-PP hollow fiber.

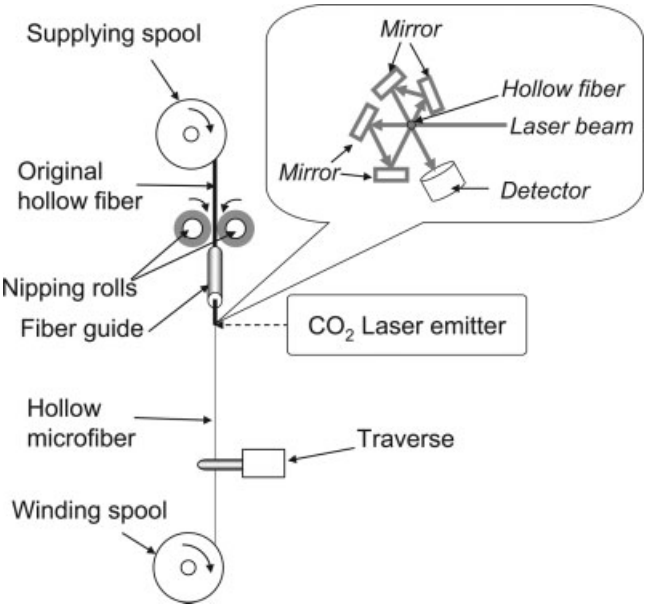

Figure 3 Schematic diagram of apparatus used for laser-thinning of hollow fiber.

CO_2 laser-thinning apparatus

The CO_2 laser-thinning apparatus to stably and continuously produce the hollow microfiber consists of supplying and winding motors with spools, a continuous wave CO_2 laser emitter, supplying system composed of a fiber guide and nipping rolls, a optical system, and a traverse as shown in Figure 3. The optical system to circularly irradiate the laser to the original hollow fiber was composed of four mirrors as shown in Figure 3. The continuous wave CO_2 laser emitted light at 10.6 μm, and the laser beam was a 4.0 mm diameter spot. A laser power was measured by the power meter during the laser-irradiating. The laser power density (PD) was estimated by dividing the measured laser power in the area of the laser spot. The laser power of more than 90% is obtained in the area of the laser spot. The laser with the PD range of 6–9 W cm^{-2} was irradiated to the hollow fiber. It is necessary to supply the original hollow fiber to a laser irradiating point at a constant speed and to circularly irradiate the CO_2 laser to stably prepare the hollow microfiber. The supplying system pulls out the original hollow fiber of the supplying spool and supplies it to the laser irradiating point at a constant speed. The supplying system and the optical system play an important role in the CO_2 laser-thinning apparatus. The hollow microfiber thinned at the laser irradiating point is wound up on the spool in the winding speed range of 100–2500 m min^{-1}. Draw ratio can be calculated easily using the following equation:

$$\text{Draw ratio} = (\text{winding speed}/\text{supplying speed}).$$

Drawing of hollow microfiber

The bundle hollow microfibers obtained by the laser-thinning were drawn at 23°C and a relative humidity of 50% with EZ Graph (Shimadzu, Kyoto, Japan). A gauge length of 30 mm and elongation rate of 10 mm min^{-1} were used.

RESULTS AND DISCUSSION

CO_2 laser-thinning of hollow fiber

Figure 4 shows the winding speed (S_w) dependence of the OD and ID for the hollow microfibers obtained at two different supplying speeds (S_s). The OD and ID of the microfiber obtained at each S_s decrease with increasing S_w. The obtained hollow microfibers when the microfiber prepared by irradiating the laser to the original fiber supplied at S_s = 0.30 m min^{-1} was wound up at S_w = 800 m min^{-1}, and the thinnest hollow microfiber with ID = 2.2 and OD = 6.3 μm was obtained, and its draw ratio reaches 2667-fold.

Figure 5 shows the SEM photographs for the hollow microfibers wound up at various S_ws when the original hollow fiber was supplied at 0.3 and 0.6 m min^{-1}. The cross section of the hollow microfiber was deformed by the cutting of the hollow microfiber. The degree of deformation in the cross section increased with decreasing the hollow fiber's diameter, because its strength decreased as fiber's diameter decreased. However, the observation by the SEM photographs shows that the hollow microfibers have the tube wall with a uniform thickness.

Figure 6 shows the SEM photographs of the necks of hollow fibers obtained at four different S_ws. The spindle-shaped neck formed at the laser-irradiating

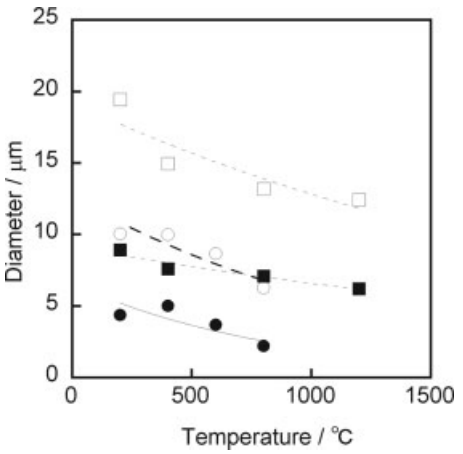

Figure 4 Winding speed dependence of an outside diameter (OD) and an internal diameter (ID) for hollow fibers obtained at two different supplying speeds (S_s): ○, OD (S_s = 0.3 m min^{-1}); ●, ID (S_s = 0.3 m min^{-1}); □, OD (S_s = 0.6 m min^{-1}); ■, ID (S_s = 0.6 m min^{-1}).

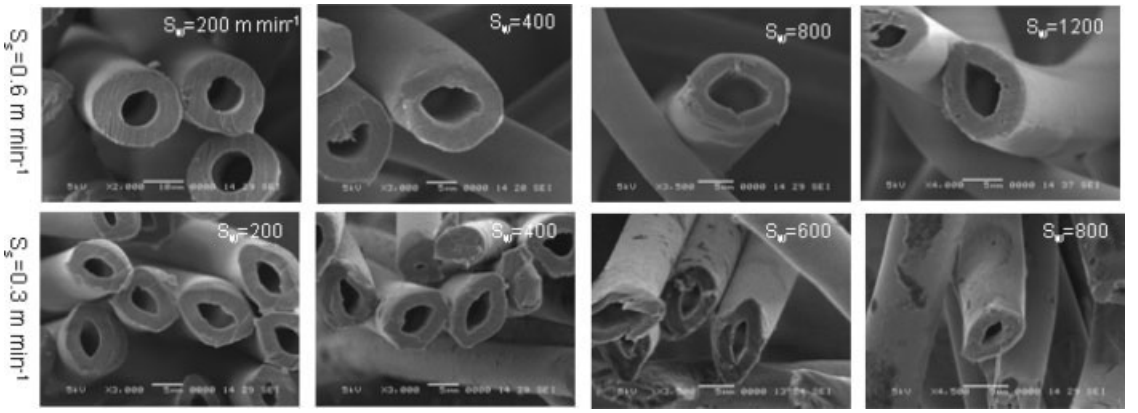

Figure 5 SEM photograph of i-PP hollow microfibers obtained at various winding speeds (S_w) at supplying speeds (S_s) of 0.3 and 0.6 m min^{-1}.

point suggested that the laser-thinning was instantly induced by the plastic flow from the nearly molten state. The hollow microfiber was not occluded by the melting induced by the laser-irradiation, and the hollow structure was maintained.

Figure 7 shows the S_w dependence of the h for hollow microfibers obtained at two different S_ss. The h value at each S_s decreased with increasing the S_w after the h value passed through maximum value. However, the hollow structure with uniform wall thickness was maintained, although the h value decreased by the laser-thinning. The decrease of the h value suggests that thinning of the hollow microfiber at the higher S_w was induced not only by the plastic flow but also by the thermal shrinkage in cross section.

Figure 8 shows equatorial wide-angle X-ray diffraction (WAXD) in intensity and the WAXD patterns of the hollow microfibers wound up at four different winding speeds. The hollow microfibers obtained have three strong equatorial reflections [$(\underline{1}10)$, (040), and (130)], and two reflections [(041) and $(\bar{1}3\bar{1})$]. The sharpening of the diffraction spot indicates an improvement in crystal perfection and an increase in the degree of crystal orientation and the crystal size. This fact indicates that not only the molecular flow but also the molecular orientation and crystallization are induced by the higher strain rate during the thinning process.

The i-PP crystallizes in three polymorphic forms: α-monoclinic, β-hexagonal,[17–19] and γ-orthorhombic crystal forms.[20,21] The α form is the most stable crystalline phase and can be easily obtained by crystallization from the melt or from solution.[22] The α form is further classified in two limiting modifications, that is, α_1 and

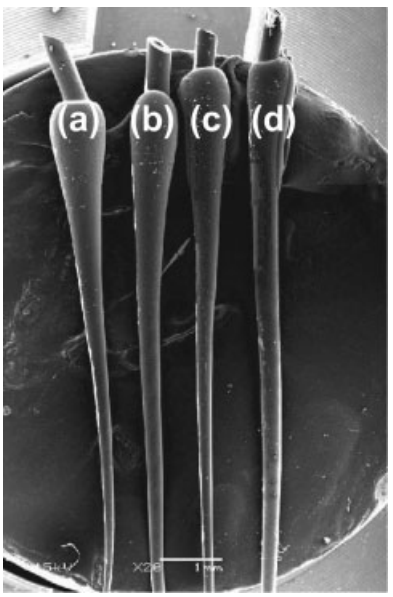

Figure 6 SEM photographs of the necks of hollow fibers obtained at four different winding speeds (S_w): (a) S_w = 1200 m min^{-1}, (b) S_w = 800 m min^{-1}, (c) S_w = 400 m min^{-1}, (d) S_w = 200 m min^{-1} (at a supplying speed of 0.6 m min^{-1}).

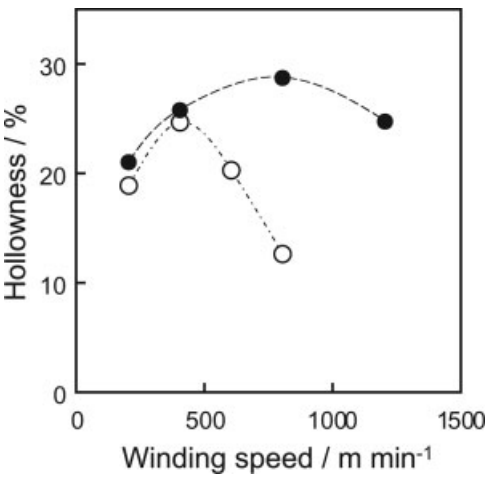

Figure 7 Winding speed dependence of the hollowness for hollow microfibers obtained at two different supplying speeds (S_s): ○, S_s = 0.3 m min^{-1}; ●, S_s = 0.6 m min^{-1}.

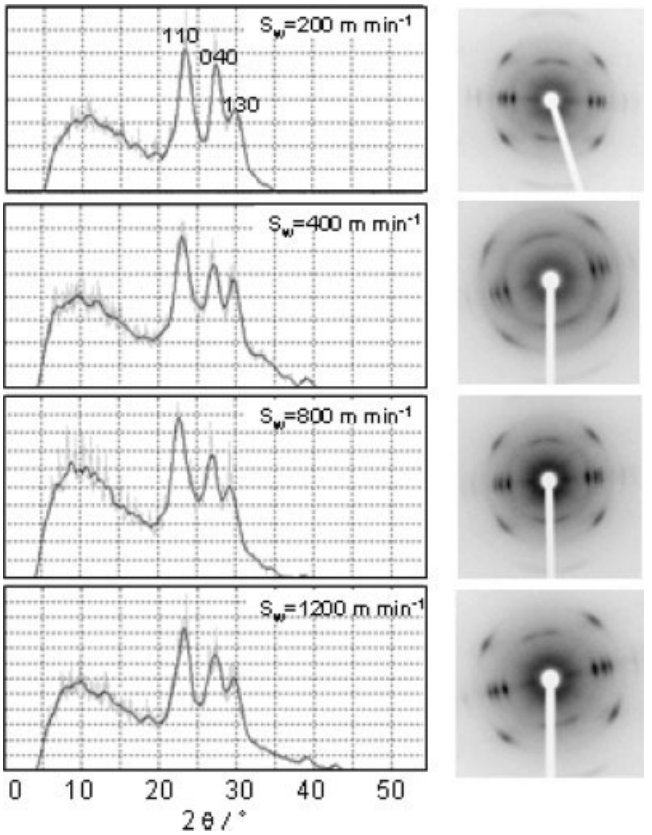

Figure 8 Equatorial wide-angle X-ray diffraction (WAXD) in intensity and the WAXD patterns of the hollow microfibers wound up at four different winding speeds (at a supplying speed of 0.6 m min^{-1}).

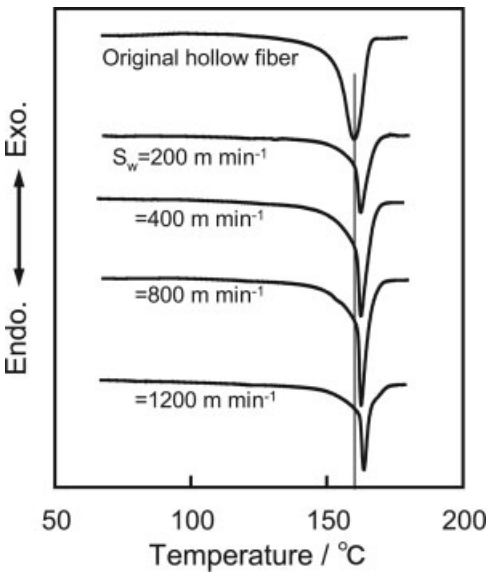

Figure 9 DSC curves for the original hollow fiber and the hollow microfibers wound up at four different winding speeds (at a supplying speed of 0.6 m min^{-1}).

α_2.[23,24] The α_1 form is characterized by a statistical disorder like that described for the space group C2/c. The α_2 form is characterized by regularity of up and down positioning of the chains, as in the space group $P2_1/c$.

Both the α_1 and α_2 forms have substantially identical X-ray spectra. However, while only reflections with $(h + k)$ even are allowed in the α_1 form, reflections with $(h + k)$ odd may be present in the α_2 form.[25] All reflections observed are reflections with $(h + k)$ even. It is known that the β form exhibits a strong equatorial reflection (300) at $2\theta = 16.10^\circ$, and that γ form[26] is observed (113) at $2\theta = 14.98^\circ$ and (117) at 20.06°. However, no reflections due to the β and γ form are observed in Figure 8. Therefore, these wide-angle X-ray diffraction photographs show that only α_1 form exists in the microfibers. The results obtained are very much in agreement with the results of the DSC measurements that will be described below.

Table I lists the degree of crystal orientation (π) for the original hollow fiber and the hollow microfibers obtained by the laser-thinning at various winding speeds. The π value reached about 90%, although the laser-thinned fiber was obtained by an instantaneous plastic flow from the nearly molten state. The existence of the highly-oriented crystallites suggested that the large deformation occurring after the laser heating induces the molecular orientation and the strain-induced crystallization.

Figure 9 shows DSC curves for the original hollow fiber and the hollow microfibers wound up at four different winding speeds, and Table II lists the melting temperature (T_m), heat of fusion (ΔH_m), and degree of

TABLE I
Degree of Orientation of Crystallites for the Original Hollow Fiber and the Hollow Fibers Obtained by the Laser-Thinning At Various Winding Speeds (S_w)

Fiber	π (%)
Original hollow fiber	67
S_w	
200 m min^{-1}	91
400 m min^{-1}	88
800 m min^{-1}	89
1200 m min^{-1}	93

TABLE II
Melting Temperature (T_m), Heat of Fusion (ΔH_m), and Degree of Crystallinity (X_c) for the Original Hollow Fiber and the Hollow Fibers Obtained by the Laser-Thinning at Various Winding Speeds (S_w)

Fiber	T_m (°C)	ΔH_m (J g^{-1})	X_c (%)
Original hollow fiber	160.1	67.27	45.9
S_w			
200 m min^{-1}	162.4	71.33	48.7
400 m min^{-1}	162.5	73.00	49.8
800 m min^{-1}	162.6	75.91	54.8
1200 m min^{-1}	163.6	66.83	45.6

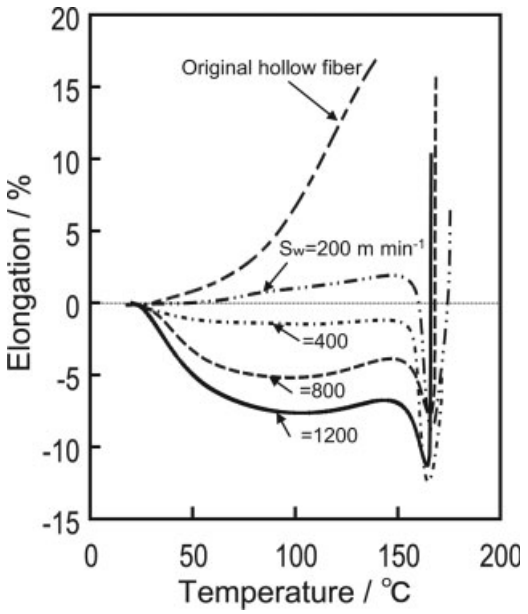

Figure 10 TMA curves of the original hollow fiber and the hollow microfibers wound up at various winding speeds.

crystallinity (X_c) estimated from the ΔH_m. The original hollow fiber has the single melting endotherm peak at 160.1°C. The T_m increased slightly as the S_w increased, and that of the hollow microfiber wound up at 1200 m min^{-1} has the single melting endotherm peak at 163.6°C. The higher the S_w, the higher is the T_m. The melting peak becomes sharp with increasing the T_m. Its sharpening is caused by an increase in the degree of perfection of the crystallites.[27,28]

The melting behavior of i-PP crystallized in different ways has been studied by several workers.[29–35] An endotherm peaking at 161°C is due to the melting of the α_1 form, and the high endotherm peaking above 170°C is due to the melting of α_2 form.[32] Jacoby et al.[24] reported that the melting endotherm due to the melting of β form was observed at about 150°C.

These DSC curves obtained have only the single melting endotherm peak around 160°C, but no melting endotherm peaks at 150 and 170°C are observed. It means, therefore, that all melting peaks are due to the melting of the α_1 form, and that no melting endotherm peaks due to the β and α_2 forms are observed. The results obtained agree well with the results of the wide-angle X-ray diffraction as mentioned above.

The X_c value increased as the S_w increased up to S_w = 800 m min^{-1}, but slightly decreased at S_w = 1200 m min^{-1}. The X_c value of the hollow microfiber obtained by the laser-thinning were lower than that (X_c = about 70%) of the zone-drawn i-PP fiber reported previously. The high winding speeds inhibited the crystallization because of a very short heating time and rapid cooling at the laser-irradiating point.

Figure 10 shows the TMA curves of the original hollow fiber and the hollow microfibers wound up at various winding speeds. The TMA behavior during heating is associated with the chain coiling in the oriented amorphous regions and is dependent on degree of amorphous orientation and the degree of crystallinity. The original hollow fiber stretched as the temperature increased. The rapid stretch with the temperature shows that no physical network, which was built up by the crystallites, preventing the fluid-like deformation exists. The hollow microfiber wound up at S_w = 200 m min^{-1} stretched gradually in the temperature range of 25–150°C, shrank rapidly, and then drastically stretched near the T_m. The peak near the T_m suggested that the physical network was broken by the melting of crystallites, and that the fluid-like deformation occurred. The hollow microfibers at S_w = 400, 800, and 1200 m min^{-1} stretch with increasing temperature and have the sharp peaks near the T_m due to the breakdown of the physical network. The thermal shrinkage in the temperature range of 25–150°C depended on the S_w, the higher S_w, the larger is the thermal shrinkage. The hollow microfiber wound at the S_w = 1200 m min^{-1} exhibited the largest thermal shrinkage due to not only highly oriented amorphous chains but also the lower degree of crystallinity compared with the hollow microfibers obtained at the other S_ws. This TMA behavior shows that the degree of amorphous orientation increased as the S_w increased, but that the crosslink density of the physical network due to the crystallites did not increased.

Figure 11 shows the temperature dependence of the DSC and the TMA curves for the hollow microfiber wound at 800 m min^{-1}. The melting peak agrees well with the TMA peak, which shows the breakdown of the physical network due to melting of the crystallites. The fact suggests that the physical network constructed

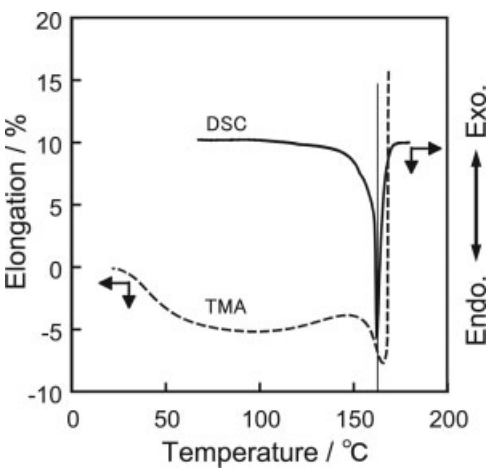

Figure 11 Temperature dependence of the DSC and the TMA curves for the hollow microfiber wound at 800 m min^{-1} (at a supplying speed of 0.6 m min^{-1}).

in the hollow microfiber supports the applied stress until immediately before when the physical network was broken by the melting of crystallites. It is well known that the mechanical properties are supported by the physical network built up the crystallites.

Drawn hollow microfiber

Figure 12 shows draw ratio dependence of the OD, ID, and hollowness for hollow microfibers drawn at various draw ratio. The hollow fiber used in the drawing had OD = 20.1, ID = 8.9 μm, and a hollowness of 20%. The OD and ID decreased, and the hollowness increased as the draw ratio increased. The wall thickness decreased with increasing draw ratio. The hollow microfiber drawn at five times had OD = 10.7, ID = 6.6 μm, and a hollowness of 34%.

Figure 13 shows the WAXD patterns of the hollow microfibers drawn at a draw ratio of five times. Three strong equatorial reflections [(110), (040), and (130)], and two reflections [(041) and ($\bar{1}3\bar{1}$) become sharper than those of the laser-thinned hollow microfibers as shown in Figure 8. The sharpening of the diffraction spot indicates an improvement in crystal perfection and an increase in the degree of crystal orientation and the crystal size.

CONCLUSIONS

The CO_2 laser-thinning method was applied to the i-PP hollow fiber to obtain the hollow microfiber. The ID and OD decreased with increasing winding speed, and its hollowness decreased slightly when comparing with the original one. In spite of the laser-thinning due to the partial melting induced by the laser-irradiation, the hollowness was hold, and such hollow structure will not be able to be made by any conventional spinning. As the microfibers are fit for various purposes, many applications of the hollow microfiber will be found in medical and industrial fields.

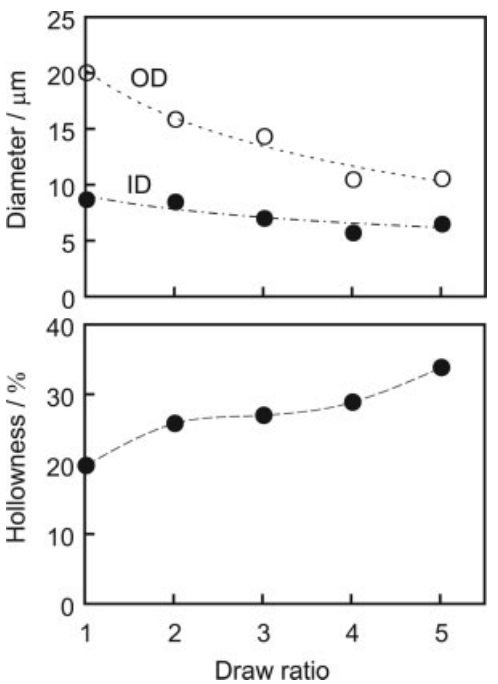

Figure 12 Draw ratio dependence of an outside diameter (OD), an internal diameter (ID), and hollowness for hollow microfibers drawn at various draw ratios: ○, OD; ●, ID.

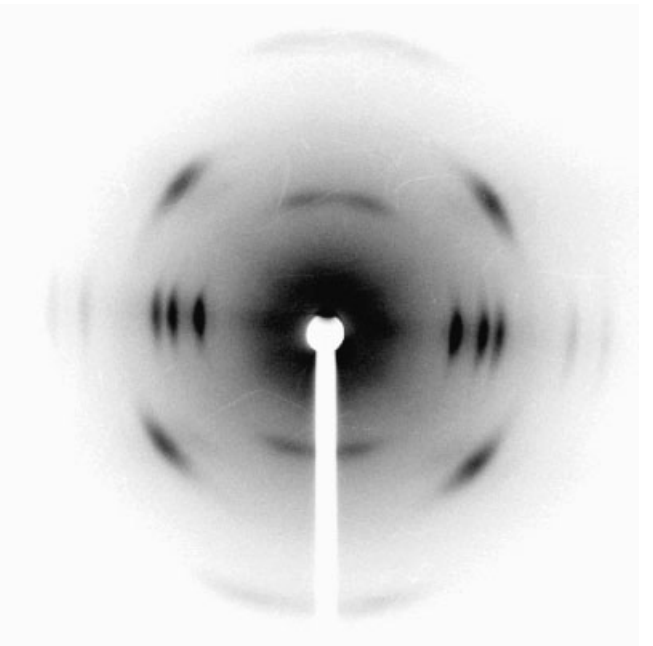

Figure 13 Wide-angle X-ray diffraction pattern of the hollow microfiber drawn at a draw ratio of five times.

References

1. Lee, M. S.; Kim, S. Y. J Appl Polym Sci 2001, 81, 2170.
2. Hsiao, K. J.; Jen, Z. F.; Lu, C. L. J Appl Polym Sci 2002, 86, 3601.
3. Sonnenschein, M. F. J Appl Polym Sci 1999, 72, 175.
4. He, T.; Mulder, M. H. V.; Wessling, M. J Appl Polym Sci 2003, 87, 2151.
5. Mei, L.; Zhang, D.; Wang, Q. J Appl Polym Sci 2002, 84, 1390.
6. Lee, M. S.; Oh, H. W.; Kim, S. Y.; Shimhyun, J. J Appl Polym Sci 1999, 74, 1836.
7. Kim, J. J.; Jang, T. S.; Kwon, Y. D.; Kim, U. Y.; Kim, S. S. J Membr Sci 1994, 93, 209.
8. Bhat, G. S.; Malkan, S. R. J Appl Polym Sci 2002, 83, 572.
9. De Clerck, K.; Rahier, H.; Mele, B. V.; Kiekens, P. J Appl Polym Sci 2003, 89, 3840.
10. Zhao, R.; Wadsworth, L. C. Polym Eng Sci 2003, 42, 463.
11. Rwei, S. P. Polym Eng Sci 2004, 44, 331.
12. Suzuki, A.; Okano, T. J Appl Polym Sci 2004, 92, 2989.
13. Suzuki, A.; Kamata, K. J Appl Polym Sci 2004, 92, 1454.
14. Suzuki, A. Narisue, S. J Appl Polym Sci 2006, 99, 27.
15. Suzuki, A.; Mizuochi, D.; Hasegawa, T. Polymer 2005, 46, 5550.
16. Huda, M. N.; Dragaun, H.; Bauer, S.; Muschik, H.; Skalicky, P. Colloid Polym Sci 1985, 263, 730.
17. Fujiwara, Y.; Goto, T.; Yamashita, Y. Polymer 1987, 28, 1253.

18. Tjong, S. C.; Shen, J. S.; Li, R. K. Y. Polymer 1996, 37, 2309.
19. Dorset, D. L.; McCourt, M. P.; Kopp, S.; Schumacher, M.; Okihara, T.; Lotz, B. Polymer 1998, 39, 6331.
20. Brücker, S.; Meille, S. V. Nature 1989, 340, 455.
21. Meille, S. V.; Brücker, S.; Porzio, W. Macromolecules 1990, 23, 4114.
22. Wills, A. J.; Capaccio, G.; Ward, I. M. J Polym Sci Polym Phys Ed 1980, 18, 493.
23. Hikosaka, M.; Seto, T. Polym J 1973, 5, 111.
24. Jacoby, P.; Bersted, B. H.; Kissel, W. J.; Smith C. E. J Polym Sci Polym Phys Ed 1986, 24, 461.
25. Kalay, G.; Zhong, Z.; Allan, P.; Bevis, M. J. Polymer 1996, 37, 2077.
26. Napolitano, R. J Polym Sci Part B: Polym Phys 1990, 28, 139.
27. Natta, G.; Corradini, P. Nuovo Cimento 1960, 15 (Suppl.), 40.
28. Natta, G. J Polym Sci 1955, 16, 143.
29. Hsu, C. C.; Geil, P. H.; Miyaji, H.; Asai, K. J Polym Sci Polym Phys Ed 1986, 24, 2379.
30. Guerra, G.; Petraccone, V.; Corradini, P.; DeRosa, C.; Napolitano, R.; Pirozzi, B. J Polym Sci Polym Phys Ed 1984, 22, 1029.
31. Yadav, Y. S.; Jain, P. C. Polymer 1986, 27, 721.
32. Awaya, H. Polymer 1988, 29, 591.
33. Paukkeri, R.; Lehtinen, A. Polymer 1993, 34, 4075.
34. Paukkeri, R.; Lehtinen A. Polymer 1993, 34, 4083.
35. Vleeshouwers, S. Polymer 1997, 38, 3213.